X-ray structure analysis of an engineered Fe-superoxide dismutase Gly-Ala mutant with significantly reduced stability to denaturant

ARTICLE *in* FEBS LETTERS · JULY 1996

Impact Factor: 3.17 · DOI: 10.1016/0014-5793(96)00490-5 · Source: PubMed

7 AUTHORS, INCLUDING:

Stephen P Wood
University College London
171 PUBLICATIONS **6,607** CITATIONS

SEE PROFILE

X-ray structure analysis of an engineered Fe-superoxide dismutase Gly-Ala mutant with significantly reduced stability to denaturant

J.B. Cooper[a,*], S. Saward[a], P.T. Erskine[a], M.O. Badasso[a], S.P. Wood[a], Y. Zhang[b], D. Young[b]

[a]*Department of Crystallography, Birkbeck College, University of London, Malet Street, London WC1E 7HX, UK*
[b]*Department of Medical Microbiology, Wright Fleming Institute, St. Mary's Hospital Medical School, Imperial College of Science, Technology and Medicine, University of London, London W2 1PG, UK*

Received 21 March 1996; revised version received 29 April 1996

Abstract **We have refined the X-ray structure of a site-directed G152A mutant of the iron-dependent superoxide dismutase from *Mycobacterium tuberculosis* at 2.9 Å resolution. The mutation which replaces a glycine residue in a surface loop with alanine was designed to alter the conformation of this loop region which has previously been shown to play a crucial structural role in quaternary interactions within the SOD tetramer. Gly-152 was targeted as it has dihedral angles ($\phi = 83.1°$, $\psi = -0.3°$) close to the left-handed α-helical conformation which is rarely adopted by other amino acids except asparagine. Gly-152 was replaced by alanine as it has similar size and polarity, yet has a very low tendency to adopt similar conformations. X-ray data collection on crystals of this mutant at 2.9 Å resolution and subsequent least-squares refinement to an *R*-value of 0.169 clearly establish that the loop conformation is unaffected. Fluorescence studies of guanidine hydrochloride denaturation establish that the mutant is 4 kcal/mol less stable than the wild-type enzyme. Our results indicate that strict conformational constraints imposed upon a region of polypeptide, due for example to interactions with a neighbouring subunit, may force an alanine residue to adopt this sterically hindered conformation with a consequent reduction in stability of the folded conformation.**

Key words: Superoxide dismutase; *Mycobacterium tuberculosis*; X-ray structure; Site-directed mutagenesis

1. Introduction

The *Mycobacterium tuberculosis* superoxide dismutase is a 207 residue enzyme with a subunit molecular weight of 23 kDa [1]. It is one of a homologous series of superoxide dismutases (SODs) with α+β tertiary structure which have either iron or manganese located at the catalytic centre and can be either dimeric or tetrameric. X-ray structures for several other members of this family are available: human [2], *B. stearothermophilus* [3], *E. coli* [4], *P. ovalis* [5] and *T. thermophilus* [6]. These enzymes are structurally distinct from the Cu-Zn family of SODs which form β-barrel dimers. The active site residues of Fe- and Mn-SODs are almost completely conserved, the metal being ligated by three histidine side chains and one aspartate carboxyl which are surrounded by a shell of aromatic residues. The subunits of all Fe- or Mn-SODs associate to form structurally conserved dimers such that residues close to the active site in one subunit interact with the metal binding residues of the other monomer thereby maintaining the metal ions at an approximate distance of 18 Å.

The structure of the *M. tuberculosis* SOD has recently been determined at 2.0 Å resolution [7] establishing that it is a compact tetramer with extensive dimer-dimer interactions involving a helical hairpin in its N-terminal domain and a loop region (144–152) which diagonally crosses the three membered β-sheet in the C-terminal domain. A diagram of the tertiary structure of the *M. tuberculosis* SOD is shown in Fig. 1 where the two regions which dominate the dimer-dimer quaternary interactions are indicated. Comparison of the dimer-dimer contacts within the tetrameric members of this family shows that they vary greatly from enzyme to enzyme [7,8]. In *T. thermophilus* SOD the dimers associate quite loosely by interactions involving residues of the helical hairpin and residues in the loop (144–152 in *M. tuberculosis* numbering) which links the two outer strands of the β-sheet in the adjacent dimer [6]. In contrast, the dimers of the human mitochondrial SOD associate more tightly by virtue of extensive interactions between the helical hairpins of adjacent subunits [2,8] which give rise to four-helix bundle structures. In the *M. tuberculosis* SOD, the dimers associate such that the 144–152 loops of adjacent subunits interact extensively at the dimer-dimer interface where they are disposed around one of the tetramer two-fold axes. Other interactions at the dimer-dimer interface involve the helical hairpin of the first domain which associates with residues 106–118 in an α-helix and the 144–152 loop of the neighbouring dimer. Hence, in all the tetrameric SODs, it is clear that the helical hairpin and the 144–152 loop dominate the dimer-dimer interactions even though the resulting quaternary structures can be very different. These two regions are where the SODs differ greatly in terms of sequence and local structure. In the human and *M. tuberculosis* SODs the helical hairpin forms a straight, projecting element of supersecondary structure whereas in the dimeric enzymes it is greatly distorted and associates with the 144–152 loop of the same subunit. Hence, it appears that in the dimeric SODs, the two regions which are otherwise important for tetramer formation appear to interact with each other, thereby preventing potential interactions with a neighbouring dimer. It therefore follows that residue substitutions in the helical hairpin and the 144–152 region may have a pivotal effect on the quaternary structure and stability of the tetramer. Our objective was to test this hypothesis by site-directed mutagenesis.

Residues 150–153 of the mycobacterial enzyme adopt a conformation close to that of type II reverse turns. These invariably have a glycine at the i+2 position because the flexibility of this amino acid allows it to adopt the required

*Corresponding author. Fax: (44) (171) 631-6803.

PII S0014-5793(96)00490-5

conformation with both ϕ and ψ positive. The equivalent residue in the mycobacterial SOD is Gly-152 which has ϕ and ψ angles of 83.1° and −0.3°, respectively, and is close to the left-handed helical conformation. We anticipated that mutating this residue to one with a low tendency to adopt the α_L-conformation could significantly disrupt the conformation of the loop with potential consequences for the quaternary structure of the tetramer. Alanine was chosen as it has minimal tendency to occur in the α_L-conformation [9] and has similar size and polarity to glycine, thereby minimising the chance of disrupting the folding and expression level of the mutant protein.

2. Materials and methods

2.1. Mutagenesis, expression and purification of M. tuberculosis SOD

A polymerase chain reaction-based (PCR) site-directed mutagenesis approach [10] was used to generate the Gly-152→Ala mutation in *M. tuberculosis* SOD using the construct pYZ8 (pUC19+1.1 kb *EcoRI*/*KpnI* fragment containing the SOD gene). The mutant forward primer Y200 (25-mer) to change Gly-152 (GGC) to Ala (GCC) based on the *M. tuberculosis* SOD DNA sequence [1] was 5′-TCCCGCTAGCCATTGTTCCGCTGCT-3′. The mutant reverse primer Y201 (25-mer) was 5′-GAACAATGGCTAGCGGAAGTTCGT-3′. In both cases the mutated nucleotides are underlined. The PCR-based site-directed mutagenesis used required two rounds of PCR reaction. The first round of PCR consisted of two independent PCR reactions. The first PCR reaction was performed with an M13/pUC universal primer and the mutant reverse primer Y201, and the second reaction was carried out with mutant forward primer Y200 and the M13/pUC reverse primer. The PCR was run using the following parameters: 95°C for 3 min, followed by 25 cycles of 95°C 1 min, 60°C 1 min, 72°C 1.5 min. Because the two mutant primers overlap, the second round of PCR was performed under the same conditions as above after mixing the two PCR products from the first round of PCR in one tube.

The PCR product from the second PCR was then cloned into the PCR-Script vector (Stratagene) and positive clones were identified by restriction analysis of the plasmid preparation with *KpnI*. Positive clones gave a single 1.1 kb *KpnI* fragment containing the putative mutant *M. tuberculosis* SOD gene, as both the PCR product and the cloning vector contained a *KpnI* site. The 1.1 kb *KpnI* fragment was then ligated into the *KpnI* site of the hygromycin mycobacterial shuttle vector p16R1 [11] and transformed into *E. coli* strain XL1-blue. Positive clones were similarly identified with *KpnI* digestion and electroporated into *M. vaccae* together with a vector control as described in [1]. The protein extracts from the *M. vaccae* transformants were then analysed by SOD activity gel and SDS-PAGE as described previously [1]. The mutant *M. tuberculosis* SOD was then purified as described by [12].

2.2. Crystallisation, data collection and structure determination

Crystals were grown at 4°C by the hanging drop method under similar conditions to the native enzyme [12] using a protein concentration of 3.0 mg/ml mixed in a 1:1 ratio with, and equilibrated against, well solutions of 25–31% PEG 6000 in 100 mM Tris-HCl buffer in the pH range 6.6–7.6. Two X-ray data sets were collected from small crystals maintained at 4°C, one at station 9.5 at the Synchrotron Radiation Source (Daresbury, UK) using a wavelength of 0.92 Å and the other at station BW6 at the DORIS ring of Deutsches Elektronen Synchrotron (Hamburg) using a wavelength of 0.96 Å. Both data sets were collected to a maximum resolution of 2.9 Å using MAR research image plate detectors and processed by the MOSFLM program [13].

The structure of the mutant was solved by the difference Fourier method [14] using the CCP4 suite of programs [15] and was refined using all data stronger than $2\sigma(F)$ to the limiting resolution of the data (2.9 Å). Refinement of all atomic coordinates and isotropic temperature factors of a single 'average' subunit was performed using the rigid-body and non-crystallographic symmetry averaging options of RESTRAIN [16] interspersed with graphics remodelling using O [17] implemented on Silicon Graphics machines.

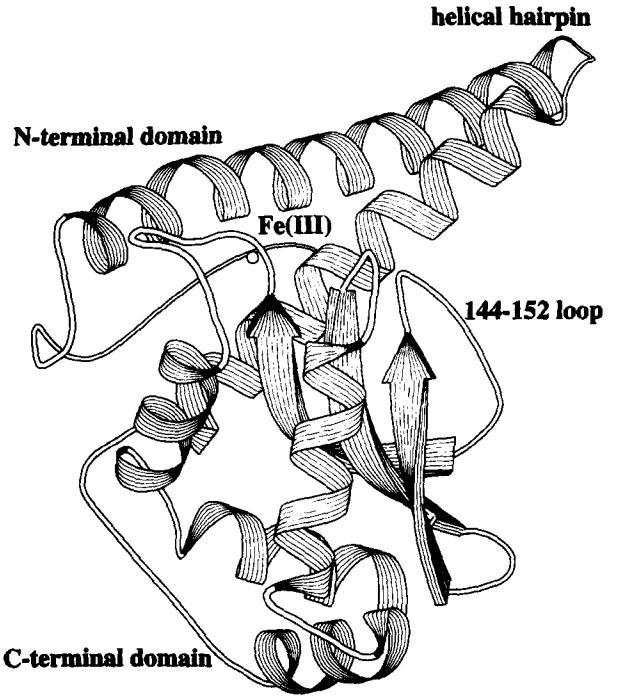

Fig. 1. A ribbon diagram of the tertiary structure of the superoxide dismutase from *Mycobacterium tuberculosis*. The helical hairpin in the N-terminal domain and the 144–152 loop region in the C-terminal domain, both of which play crucial roles in the dimer-dimer interactions, are indicated.

2.3. Guanidine hydrochloride denaturation

Fluorescence spectra of the mutant and wild-type SOD were recorded at 296 K with a Shimadzu RF-5000 fluorescence spectrophotometer by exciting the sample at 280 nm and recording the intrinsic fluorescence from 300 to 400 nm. The enzyme was diluted into a series of Gu·HCl solutions ranging from 0.0 M to 6.0 M buffered with 200 mM Tris·HCl at pH 7.9 with an enzyme concentration of 1 μM. Unfolding was allowed to proceed for 24 h prior to recording the spectra which were smoothed and had the guanidine background subtracted. The extent of unfolding was measured from the fluorescence at 366 nm where the difference spectrum between unfolded and folded enzyme had the largest peak. The equilibrium constant for unfolding K_U (F (folded)⇌U (unfolded); $K_U = [U]/[F]$) was calculated from the ratio $(F-F_F)/(F_U-F)$ where F = fluorescence at 366 nm, F_F = fluorescence of the folded form at 366 nm and F_U = fluorescence of the unfolded form in 6.0 M Gu·HCl at 366 nm. The corresponding ΔG_U values (obtained from $\Delta G_U = -RT\ln K_U$) were analysed according to the equation $\Delta G_U = \Delta G_u^\circ - m[\text{denaturant}]$ with ΔG_U° being obtained by extrapolation to zero guanidine concentration. The parameter m is a measure of the cooperativity of the transition [18]. The reversibility of unfolding was tested by dialysis to remove the denaturant followed by recording the fluorescence and an activity assay [19].

3. Results

The substitution of Ala for Gly at position 152 was confirmed by DNA sequencing. Previously we showed that *M. tuberculosis* SOD was highly expressed by its own promoter in another mycobacterium, *M. vaccae* [11]. In the current experiment, the G152A mutant SOD was similarly transformed into *M. vaccae* and analysed by SDS-PAGE and SOD activity gels. SOD activity gel analysis [19] revealed that the mutant *M. tuberculosis* SOD possessed strong activity, with three other weaker SOD bands possibly due to hy-

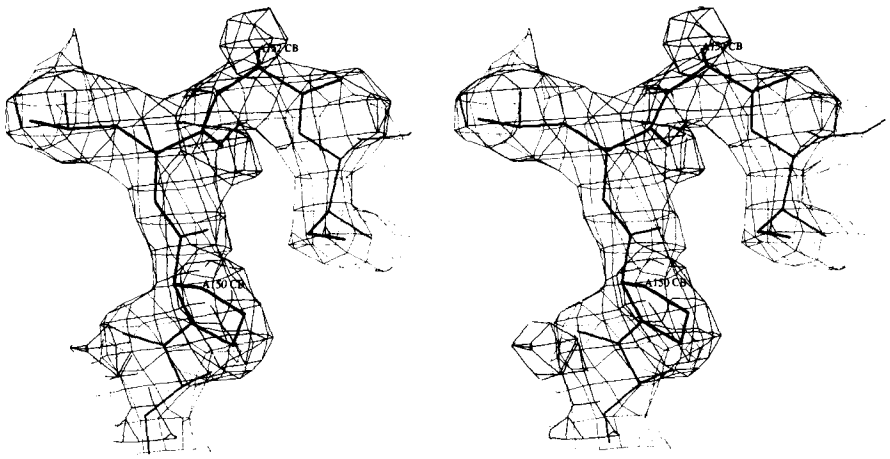

Fig. 2. A stereo view of the electron density ($2F_O$-F_C) contours for the Ala-152 residue in the G152A mutant structure.

hrid tetramers formed between *M. tuberculosis* mutant SOD and the *M. vaccae* SOD subunits.

The crystals of the G152A SOD mutant were found to be isomorphous with those of wild-type enzyme which belong to the $P2_1$ space group. X-ray crystallographic data for the mutant enzyme are shown in Table 1 along with the stereochemical residuals for the refined structure. A final refinement *R*-factor of 0.169 and correlation coefficient of 0.927 were obtained. The geometry of the model is acceptable by the PROCHECK criteria [20] having 89% of residues within the 'most favoured' regions of the Ramachandran plot. Isotropic temperature factors for 1569 protein atoms in the subunit and 92 'heteroatoms' (water molecules and the iron) refined to mean values of 12.2 Å^2 and 31.0 Å^2 which are reasonable for a 2.9 Å resolution data set.

In the G152A structure the electron density is extremely well defined at the site of the mutation in all four subunits (Fig. 2). Alanine 152 has ϕ and ψ values of 70.2° and 7.9° which have changed only slightly from the values of 83.1° and −0.3° for the wild-type protein. The ϕ and ψ angles of Ala-152 are within the left-handed α-helical region which indicates that the conformation has changed minimally to adopt a sterically permissible conformation albeit with close van der Waals contacts between the Ala-152 Cβ atom and adjacent main chain carbonyl groups. However, the alanine Cβ makes two favourable van der Waals contacts (shorter than 4 Å) not present in the wild-type enzyme with the side chain oxygen of Thr-132 and with Pro-155 from the neighbouring subunit. One water molecule close to the Ala-152 side chain moves by approximately 1 Å from its position in the wild-type structure as a result of the mutation. The instability of the mutant presumably stems from close van der Waals contacts of 2.9–3.0 Å made by the side chain methyl group of residue 152 with the adjacent carbonyl oxygens of residues 151 and 152. Details of the interactions made by residue 152 in the mutant can be seen in Fig. 3.

Least-squares fitting the whole tetramer as a rigid group to the wild-type structure gave an RMS deviation of 0.20 Å which is less than the estimated RMS coordinate error of 0.3 Å obtained by the method of Read [21]. This indicates that there is no significant change in the quaternary structure as a result of the mutation.

Both mutant and wild-type Fe-SOD intrinsic fluorescence spectra exhibited a large shift in λ_{max} from 320 nm for the folded form to 350 nm for the unfolded enzyme. With increasing guanidine hydrochloride concentration the wild-type enzyme unfolds between 3.0 and 4.0 M Gu·HCl whereas the G152A mutant unfolds significantly between 2.0 and 3.0 M Gu·HCl. The ΔG_U versus [denaturant] data in Fig. 4 show that the wild-type enzyme unfolds with a ΔG_U^o of 6.0 (±0.4)

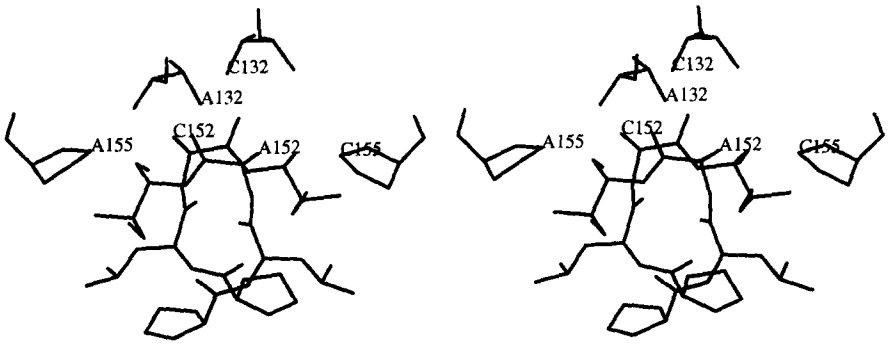

Fig. 3. Residues 150–153 of adjacent subunits in the G152A mutant tetramer. The side chain methyl group of Ala-152 makes favourable van der Waals contacts with the side chain oxygen of Thr-132 and with Pro-155 in the adjacent subunit. The atoms forming these interactions are labelled by the residue number preceded by the chain identifier (A or C). In addition, the alanine Cβ makes close contacts of around 3.0 Å with the carbonyl groups of the same residue and the preceding one.

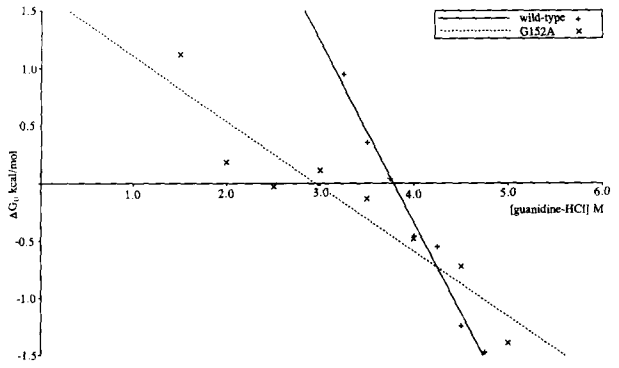

Fig. 4. A graph of ΔG_U versus [Gu·HCl] for the wild-type (solid line +) and G152A mutant (dashed line x) SOD. The vertical intercepts define the ΔG_U^o values of 6.0 (±0.4) kcal/mol for wild-type enzyme and 1.7 (±0.3) kcal/mol for the mutant.

kcal/mol whereas the mutant enzyme has a ΔG_U^o of 1.7 (±0.3) kcal/mol. In addition the unfolding transition for wild-type enzyme (m = 1.6) was found to be significantly more cooperative than for the G152A mutant (m = 0.6). Fluorescence spectra recorded after dialysis to remove denaturant confirmed that the unfolding transition is reversible and the refolded enzyme was found to have catalytic activity.

4. Discussion

We have demonstrated that mutation of glycine to alanine at position 152 of the tetrameric Fe-SOD from *M. tuberculosis* destabilises the protein and also reduces the cooperativity of the unfolding transition. The mutation is in a loop which takes part in extensive quaternary interactions between structurally conserved dimers. Replacement of glycine with a positive ϕ angle by alanine is a rare substitution in nature, by far the most common replacement being asparagine which can form a hydrogen bond involving its side chain and the local main chain to compensate for unfavourable van der Waals interactions. The Fe-SOD tetramer has accommodated the G152A substitution with minimal changes in conformation but the resulting structure is 4 kcal/mol less stable than the wild-type enzyme. Glycine to alanine substitutions have been reported to increase protein stability, an effect attributed to the reduced entropy of the unfolded state although the effects on ΔG_U^o are rather small ($\Delta\Delta G_U^o = 0.4$ kcal/mol) [22]. The substantial change in ΔG_U^o for the G152A mutant reported here presumably reflects the tightly constrained environment of the 144–152 loop at the dimer-dimer interface.

Table 1
Refinement details of the *M. tuberculosis* SOD G152A mutant at 2.9 Å

Unit cell parameter	
a	68.7 Å
b	85.6 Å
c	66.7 Å
β	99.8°
Space group	$P2_1$
No. molecules/asymmetric unit	4
Solvent content	41%
Completeness of reflection data set to 2.9 Å resolution	88.2%
Percentage of reflections with $I > 3\sigma(I)$	64.9%
Merging *R*-factor of the data to 2.9 Å	15.4%
Mean multiplicity to 2.9 Å	4.1
No. of reflections from 20.0 Å to 2.9 Å	14468 ($2\sigma(F)$ cutoff)
No. of refinement restraints	4171
No. of parameters refined	6647
R-factor	0.169
Correlation coefficient	0.927
RMS deviation from ideal bond lengths	0.013 Å
RMS deviation from ideal third-atom distances	0.030 Å
RMS deviation of close contacts	0.042 Å
RMS deviation from main chain planarity	0.011 Å
RMS deviation from side chain planarity	0.009 Å

Acknowledgements: We acknowledge N. Srinivasan, I. Sumner, J. Jackson and K. Bunting for many useful discussions.

References

[1] Zhang, Y., Lathigra, R., Garbe, T., Catty, D. and Young, D. (1991) Mol. Microbiol. 5, 381–391.
[2] Borgstahl, G.E.O., Parge, H.E., Hickey, M.J., Beyer, W.F., Jr., Hallewell, R.A. and Tainer, J.A. (1992) Cell 71, 107–118.
[3] Parker, M.W. and Blake, C.C.F. (1988) J. Mol. Biol. 199, 649–661.
[4] Lah, M.S., Dixon, M.M., Pattridge, K.A., Stallings, W.C., Fee, J.A. and Ludwig, M.L. (1995) Biochemistry 34, 1646–1660.
[5] Stoddard, B.L., Howell, P.L., Ringe D. and Petsko, G.A. (1990) Biochemistry 29, 8885–8893.
[6] Ludwig, M.L., Metzger, A.L., Pattridge, K.A. and Stallings, W.C. (1991) J. Mol. Biol. 219, 335–358.
[7] Cooper, J.B., McIntyre, K., Badasso, M.O., Wood, S.P., Zhang, Y., Garbe, T.R. and Young D.B. (1995) J. Mol. Biol. 246, 531–544.
[8] Wagner, U.G., Pattridge, K.A., Ludwig, M.L., Stallings, W.C. Werber, M.M., Oefner, C., Frolow, F. and Sussman J.L. (1993) Protein Sci. 2, 814–825.
[9] Richardson, J.S. and Richardson D.C. (1989) in: Prediction of Protein Structure and Principles of Protein Conformation (Fasman, G.D., Ed.) pp. 1–98, Plenum, New York.
[10] Ausubel, F., Brent, R., Kingston, R.E., Moore, D.D., Seidman, J.G., Smith, J.A. and Struhl, K. (1992) in: Short Protocols in Molecular Biology, 2nd edn., John Wiley and Sons, New York.
[11] Garbe, T.R., Barathi, K., Zhang, Y., Abou-Zeid, C., Tang, D., Mukhergee, R. and Young, D.B. (1994) Microbiology 140, 133–138.
[12] Cooper, J.B., Driessen, H.P.C., Wood, S.P., Zhang, Y. and Young, D. (1994) J. Mol. Biol. 235, 1156–1158.
[13] Leslie, A.G.W. (1992) in: Newsletter on Protein Crystallography, Daresbury Laboratory, Warrington, UK.
[14] Blundell, T.L. and Johnson, L.N. (1976) Protein Crystallography, Academic Press, London.
[15] CCP4 (1994) Acta Crystallogr. D50, 760–763.
[16] Haneef, I., Moss, D.S., Stanford, M.J. and Borkakoti, N. (1985) Acta Crystallogr. A41, 426–433.
[17] Jones, T.A., Zou, J-Y., Cowan, S.W. and Kjeldgaard, M. (1991) Acta Crystallogr. A47, 110–119.
[18] Tanford, C. (1969) Adv. Protein Chem. 23, 121–282.
[19] Beauchamp, C. and Fridovich, I. (1971) Anal. Biochem. 44, 276–287.
[20] Laskowski, R.A., MacArthur, M.W., Moss, D.S. and Thornton J.M. (1993) J. Appl. Crystallogr. 26, 283–291.
[21] Read, R.J. (1986) Acta Crystallogr. A42, 140–149.
[22] Matthews, B.W., Nicholson, H. and Beckel, W.J. (1987) Proc. Natl. Acad. Sci. USA 84, 6663–6667.